The fluid and elastic nature of nucleated cells: Implications from the cellular backscatter response

Ralph E. Baddour
Department of Medical Biophysics, University of Toronto, 610 University Avenue, Toronto, Ontario M5G 2M9, Canada
rbaddour@uhnres.utoronto.ca

Michael C. Kolios
Department of Physics, Ryerson University, 350 Victoria Street, Toronto, Ontario M5B 2K3, Canada
mkolios@ryerson.ca

Abstract: In a previous experiment [Baddour *et al.*, J. Acoust. Soc. Am. **117**(2), 934–943 (2005)] it was shown that it is possible to deduce the ultrasound backscatter transfer function from single, subresolution cells *in vitro*, across a broad, continuous range of frequencies. Additional measurements have been performed at high frequencies (10–65 MHz) on cells with different relative nucleus sizes. It was found that for cells with a nucleus to cell volume ratio of 0.50, the backscatter response was better modeled as an elastic sphere. For the cells in which the ratio was 0.33, the backscatter showed good agreement with the theoretical solution for a fluid sphere.
© 2007 Acoustical Society of America

1. Introduction

A large body of work has been published that shares the common objective of characterizing biological tissues by interrogation with ultrasound, whether it be by analysis of radio-frequency (rf) backscatter echo signals (Lizzi *et al.*, 1983) or of brightness-mode (B-mode) images (Waag, 1984). Although the advent of high-frequency, pulse-echo ultrasound devices (operating in the range of 10–65 MHz) has permitted higher resolution imaging of tissues, the associated wavelengths of sound (25–150 μm)—the resolution limit for imaging applications—are still greater than the size of most eukaryotic cells (5–30 μm, when in suspension). Nevertheless, techniques have been developed that exploit global alterations in acoustic properties, such as rf echo anisotropy (Insana *et al.*, 1991) or spectral slope (Lizzi *et al.*, 1996), to deduce average structural parameters in the size regime of cells, such as effective scatterer size or distribution. However, the actual nature of the scattering interaction at the cellular level remains not well understood. Not only is it difficult to measure acoustic scattering from single cells, due to problems with localization and low signal strength, but knowledge of the precise mechanical properties of cells, required to model the scattering process, is still an ongoing area of study.

The first successful backscatter measurement from individual cells was performed by Baddour *et al.* (2005) *in vitro* and used to evaluate a proposed model of acoustic scattering from single cells. Because of the large changes in backscatter intensity observed from cell ensembles during the process of apoptotic cell death (Kolios *et al.*, 2002, 2003), and since most of the significant gross structural changes that occur in apoptosis are related to the nucleus, it was hypothesized that the nucleus is primarily responsible for the scattering from a cell. Although the validity of the model of a cell as a simple elastic sphere with nucleuslike properties was unconvincing, this study provided a useful method to deduce the backscattering from individual subresolution scatterers. Here we show the backscatter response from two different cell types, measured using a refinement of this method, to higher frequencies, achieving a higher signal-

to-noise ratio (SNR) than in previous measurements. These new results provide evidence for the dual fluid and elastic character of cells.

2. Methods

Very sparse suspensions of cells (less than 10 000 cells/cm^3) were prepared in a degassed, dilute phosphate buffered saline (PBS) solution at room temperature, as described in Baddour *et al.* (2005). Suspensions of two different types of cells were prepared: OCI-AML-5 (Wang *et al.*, 1991), a line of human acute myeloid leukemia cells, and PC-3 (Kaighn *et al.*, 1979), a line of human prostate cancer cells. These two cell types were selected because of their significant difference in nucleus to cell volume ratios. Since time in culture was found to affect cell size (Taggart *et al.*, 2006), aliquots of both suspensions were taken on the day of the experiment for sizing by optical confocal microscopy. OCI-AML-5 cells were found to have mean nucleus and cell diameters of 9.1 and 11.5 μm, respectively (nucleus to cell volume ratio=0.50). For PC-3, nucleus and cell had respective mean diameters of 17.9 and 26.0 μm (volume ratio=0.33).

Data acquisition was performed using a VisualSonics VS40b (VisualSonics Inc., Canada) high-frequency ultrasound device using three single-element transducers, each with different resonant frequencies, f numbers, and focal lengths—20 MHz polyvinylidene fluoride: f2.35, 20 mm (VisualSonics Inc., Canada); 40 MHz polyvinylidene fluoride: f3, 9 mm (VisualSonics Inc., Canada); and 80 MHz lithium niobate: f3, 6 mm (Resource Center for Medical Ultrasonic Transducer Technology, University of Southern California). Since the device only generates short, broadband pulses with preset center frequencies, the transducers were excited with 19-, 40-, and 55-MHz pulses. The performance of the 80-MHz transducer pulsed at 55 MHz was satisfactory, with a 6-dB intensity bandwidth ranging from approximately 40 to 65 MHz. With each transducer, 30 independent sets of 255 linearly separated (30-μm spacing), raw rf echo signals (unprocessed A-scans) were acquired from both cell suspensions and then thresholded, discarding all scan lines not containing any data value greater than 80% of the maximum data value detected in all the echo signals (for that particular cell type and transducer). This threshold step, to remove empty acquisition lines and indirect cell hits, was set higher than in the previous study (Baddour *et al.*, 2005) in an attempt to obtain a higher "purity" of backscattered signals (i.e., where the scattered angle is exactly 180°). It is assumed that cells centered in the focal beam width of the transducer produce a higher amplitude echo for two reasons: any deviation from the transducer axis lowers the insonation intensity and, for spherical scatterers, scattering efficiency for the pure backscatter condition is always higher than for small angles off-axis.

Using the 10 to 30 rf signals that remain from each data set after thresholding, the backscatter transfer function (BSTF) was calculated as

$$\text{BSTF} = \left| \frac{R(\omega, r)}{R_{\text{ref}}(\omega, r)} \right|^2, \tag{1}$$

where $R(\omega, r)$ is the Fourier transform of the scattered signals from the transducer's depth of field. In this study, signals were windowed with a tight Hamming window (0.4 μs in width), centered relative to the maximum amplitude of the individual scattered pulses, prior to being Fourier transformed. $R_{\text{ref}}(\omega, r)$ is the Fourier transform of a reference measurement: the perpendicular specular reflection from a flat, polished SiO$_2$ crystal (Edmund Industrial Optics Inc., part 43424; ρ=2.20 g/cm^3, c=5720 m/s) placed at the transducer focus in degassed PBS at room temperature. It has been shown that such a measurement is a valid approximation of the transducer's electromechanical response (Szabo *et al.*, 2004).

3. Results

Figure 1 shows representative backscattered pulses from individual OCI-AML-5 and PC-3 cells. For each transducer, the incident (transmitted) pulse presented is the reference pulse. Although the amplitude scales are in arbitrary units (output from the 8-bit digital sampler in the
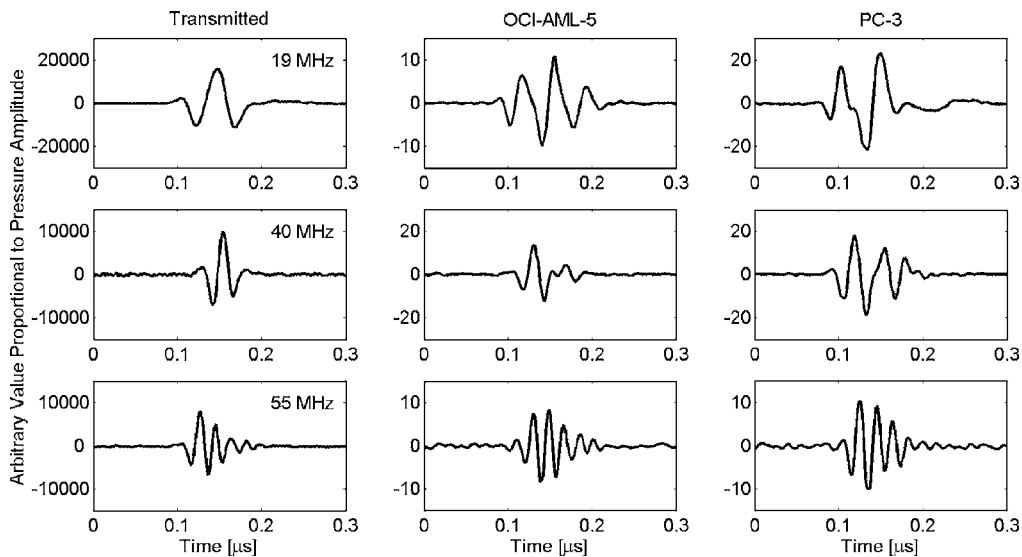
Fig. 1. Representative backscattered signals from individual cells of two different cell lines (OCI-AML-5, PC-3) and the corresponding incident acoustic pulses transmitted from three wideband transducers: an $f2.35$ 20 MHz excited at 19 MHz, an $f3$ 40 MHz excited at 40 MHz, and an $f3$ 80 MHz excited at 55 MHz.

VS40b device), all signals were corrected for gain variations and are directly comparable. It is evident from the low noise in the signals that a higher SNR was achieved compared to Baddour *et al.* (2005), where different transducers were employed; SNRs computed here (after signal thresholding) were in the range of $11-15$ dB, compared to $8-11$ dB in the previous study.

The results of the method described to deduce the BSTF from individual OCI-AML-5 and PC-3 cells is presented in the form of spectral plots [Figs. 2(a) and 3(a)]. The BSTFs, expressed in decibels relative (dBr) to the backscatter intensity from the reference, are shown for the frequency ranges corresponding to the 6-dB bandwidths of each transducer.

Four theoretical backscatter frequency responses were calculated for both cell types: elastic sphere with cell or nucleus properties, and fluid sphere with cell or nucleus properties. The Faran-Hickling solution (Faran, 1951; Hickling, 1962) was employed for the calculation of the elastic sphere responses and the Anderson solution (Anderson, 1950) for the fluid sphere responses. To generate meaningful results, reasonable values for the bulk properties of cells and their nuclei were obtained and are summarized in Table 1. Speed of sound values were obtained from recent measurements of the acoustic properties of whole cells and isolated nuclei (Taggart *et al.*, 2006). For PC-3, which were not included in these measurements, the sound speeds measured from human embryonic kidney (HEK) cells and nuclei were chosen for use here; like PC-3, HEK cells are adherent in culture and are approximately similar in size. As derived in Baddour *et al.* (2005), 1.43 g/cm^3 was used as the effective density of the nuclei. The bulk density of a whole cell was calculated as a volume-weighted sum of the nucleus density and 1.05 g/cm^3, the assumed mean density of the cytoplasm (chosen to be marginally higher than typical sea water). Finally, the Poisson's ratio (a parameter only necessary in the elastic sphere calculations) of both OCI-AML-5 and PC-3 nuclei was assumed to be the same as the one of nuclei from chondrocytes (connective tissue cells), which has been measured to be 0.42 (Knight *et al.*, 2002). For whole cells, the value of 0.487 is from experiments by Boudou *et al.* (2006) with a polyacrylamide gel developed to simulate a thin layer of cells.

Figures 2(a) and 3(a) show the theoretical frequency response of the backscatter pressure intensity that best agrees with the corresponding measured BSTF as determined by least squares analysis. To avoid figure clutter, the remaining three other theoretical solutions are pre-
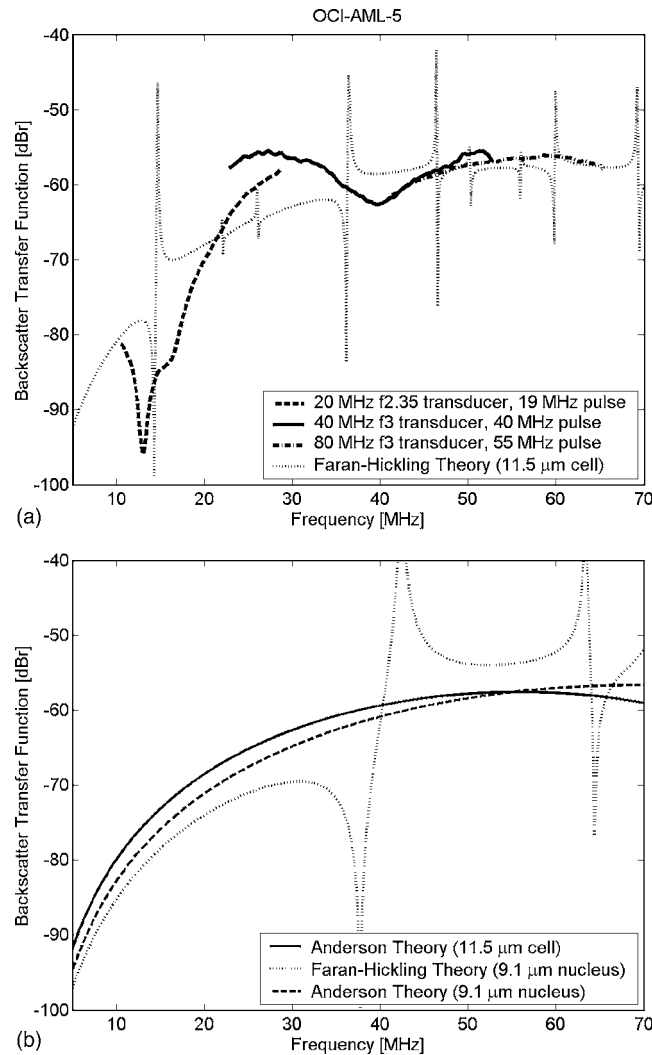
Fig. 2. Theoretical and measured backscatter frequency responses of single OCI-AML-5 cells in PBS using three different wideband transducers. (a) Measured BSTF and elastic sphere theory (properties of a whole cell). (b) Theoretical BSTFs for a fluid sphere with the properties of a whole cell, an elastic sphere with nucleus properties, and a fluid sphere with nucleus properties.

sented in Figs. 2(b) and 3(b). Note that the theoretical curves have not been shifted or scaled in any way, except to take into account the geometric effect of diminishing solid angle with distance.

4. Discussion and conclusions

The backscattered pulses from the smaller cells (OCI-AML-5) consistently had smaller peak amplitudes than those from the larger cell type (PC-3). This disparity became especially significant during 19-MHz broadband insonation. If one assumes that a PC-3 cell can best be modeled as a fluid sphere, this result is not surprising as the fundamental frequency for an air bubble in water, referred to as the Minnaert frequency if surface tension effects are disregarded (Minnaert, 1933), is $ka=0.01335$ (where a is the bubble radius and $k=\omega/c$, the incident wave number). This works out to 25 MHz for a bubble the same diameter as a PC-3 cell. Unlike the sharp
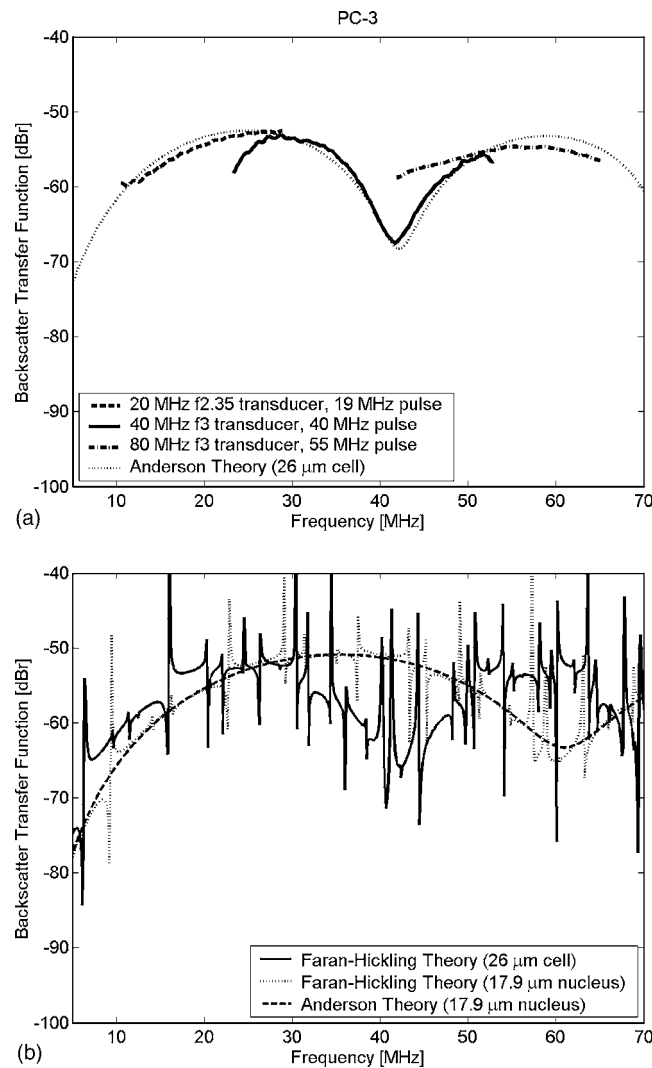
Fig. 3. Theoretical and measured backscatter frequency responses of single PC-3 cells in PBS using three different wideband transducers. (a) Measured BSTF and fluid sphere theory (properties of a whole cell). (b) Theoretical BSTFs for an elastic sphere with the properties of a whole cell, an elastic sphere with nucleus properties, and a fluid sphere with nucleus properties.

resonant peak predicted for a bubble, the theory for a liquid sphere in another immiscible liquid (a closer approximation to our experimental conditions) predicts a broader resonant response of smaller amplitude (Temkin, 1999). A rounded peak centered at 25 MHz is clearly evident in both the measured and theoretical results shown in Fig. 3(a). As can be seen in Fig. 3(b), the only other theoretical curve that predicts the measured peak in BSTF at 25 MHz is the elastic sphere whole cell theory. However, the numerous sharp resonant peaks predicted by the Faran-Hickling solution were not observed experimentally.

By visual inspection alone, it is obvious from Figs. 3(a) and 3(b) that the backscatter spectra for PC-3 cells are best fitted by the scattering theory of a fluid sphere with whole cell properties. For OCI-AML-5, the results are not as striking; the best fit appears to be with elastic sphere theory (whole cell properties). As seen in Fig. 2(a), there is some broad agreement in spectral features between the experimental BSTFs and the theoretical curve, such as the sharp

Table 1. Summary of the parameters used in the theoretical backscatter response calculations.

	Diameter d (μm)	Speed of sound c (m/s)	Density ρ (g/cm^3)	Poisson's ratio σ
OCI-AML-5 nucleus	9.1	1503	1.43	0.42
OCI-AML-5 cell	11.5	1535	1.24	0.487
PC-3 nucleus	17.9	1493	1.43	0.42
PC-3 cell	26.0	1523	1.18	0.487

dip between 10 and 20 MHz, the trough near 40 MHz, and the mean intensity level between 50 and 65 MHz. It is possible that the many sharp resonant spikes predicted by the Faran-Hickling solution might not be seen experimentally because of the normal biological variation of sizes and deviations from spherical shape for cells and nuclei in a given population, whereas the theory is defined for a geometrically perfect sphere. However, these can only be part of the cause; when the spectra from individual A-scans were examined, sharp resonances were never observed, implying the existence of additional factors.

Although analysis of the backscatter frequency response is somewhat indicative of the less fluid nature of OCI-AML-5 cells, there is further support for this hypothesis in the raw rf backscattered signals from these cells. When using a broadband 55-MHz insonation pulse (shown in Fig. 1), the scattered pulse from a typical OCI-AML-5 cell has an extent of approximately 0.1 μs and six cycles that are clearly identifiable above the noise floor. For a typical PC-3 cell, only five cycles can be identified over a similar period, although one might expect a longer backscattered signal for these cells due to their much larger size. The relatively longer backscattered pulse from the smaller OCI-AML-5 could be evidence of more elastic behavior, as elastic scatterers have a longer ring-down time.

By contrasting our analysis the ultrasonic backscatter responses measured from individual OCI-AML-5 and PC-3 cells, it is clear that the OCI-AML-5 cells behave more like elastic scatterers and that the PC-3 cells are very well modeled as fluid spheres. The results of this study imply that the nucleus behaves chiefly as an elastic scatterer and that the cytoplasm that surrounds it is well approximated by a fluid. We postulate that for cells with low nucleus to cell volume ratios (like PC-3), the effect of the nucleus is less important and the backscatter frequency response of the whole cell can best be modeled as a fluid sphere. Conversely, for cells in which the nucleus occupies a larger proportion of the cell volume (like OCI-AML-5), the elastic properties of the nucleus can no longer be ignored. It is possible that this class of cells might be best modeled as an elastic sphere surrounded by a fluid shell.

Acknowledgments

References and links

Anderson, V. C. (**1950**). "Sound scattering from a fluid sphere," J. Acoust. Soc. Am. **22**(4), 426–431.

Baddour, R. E., Sherar, M. D., Hunt, J. W., Czarnota, G. J., and Kolios, M. C. (**2005**). "High-frequency ultrasound scattering from microspheres and single cells," J. Acoust. Soc. Am. **117**(2), 934–943.

Boudou, T., Ohayon, J., Arntz, Y., Finet, G., Picart, C., and Tracqui, P. (**2006**). "An extended modeling of the micropipette aspiration experiment for the characterization of the Young's modulus and Poisson's ratio of adherent thin biological samples: Numerical and experimental studies," J. Biomech. **39**(9), 1677–1685.

Faran, J. J. (**1951**). "Sound scattering by solid cylinders and spheres," J. Acoust. Soc. Am. **23**(4), 405–418.

Hickling, R. (**1962**). "Analysis of echoes from a solid elastic sphere in water," J. Acoust. Soc. Am. **34**(10), 1582–1592.

Insana, M. F., Hall, T. J., and Fishback, J. L. (**1991**). "Identifying acoustic scattering sources in normal renal parenchyma from the anisotropy in acoustic properties," Ultrasound Med. Biol. **17**(6), 613–626.

Kaighn, M. E., Narayan, K. S., Ohnuki, Y., Lechner, J. F., and Jones, L. W. (1979). "Establishment and

characterization of a human prostatic-carcinoma cell-line (PC-3)," Investig. Urol. **17**(1), 16–23.

Knight, M. M., Bravenboer, J. V. D. B., Lee, D. A., van Osch, G. J. V. M., Weinans, H., and Bader, D. L. (**2002**). "Cell and nucleus deformation in compressed chondrocyte-alginate constructs: Temporal changes and calculation of cell modulus," Biochim. Biophys. Acta **1570**(1), 1–8.

Kolios, M. C., Czarnota, G. J., Lee, M., Hunt, J. W., and Sherar, M. D. (**2002**). "Ultrasonic spectral parameter characterization of apoptosis," Ultrasound Med. Biol. **28**(5), 589–597.

Kolios, M. C., Taggart, L., Baddour, R. E., Foster, F. S., Hunt, J. W., Czarnota, G. J., and Sherar, M. D. (**2003**). "An investigagion of backscatter power spectra from cells, cell pellets and microspheres," Proc.-IEEE Ultrason. Symp. **2003**, 752–757.

Lizzi, F. L., Greenebaum, M., Feleppa, E. J., Elbaum, M., and Coleman, D. J. (**1983**). "Theoretical framework for spectrum analysis in ultrasonic tissue characterization," J. Acoust. Soc. Am. **73**(4), 1366–1373.

Lizzi, F. L., Astor, M., Kalisz, A., Liu, T., Coleman, D. J., Silverman, R., Ursea, R., and Rondeau, M. (**1996**). "Ultrasonic spectrum analysis for assays of different scatterer morphologies: Theory and very-high frequency clinical results," Proc.-IEEE Ultrason. Symp. **1996**, 1155–1159.

Minnaert, F. M. (**1933**). "On musical air-bubbles and the sounds of running water," Philos. Mag. **16**, 235–248.

Szabo, T. L., Karbeyaz, B. U., Cleveland, R. O., and Miller, E. L. (**2004**). "Determining the pulse-echo electromechanical characteristic of a transducer using flat plates and point targets," J. Acoust. Soc. Am. **116**(1), 90–96.

Taggart, L., Baddour, R. E., Giles, A., Czarnota, G., and Kolios, M. C. (**2007**). "Ultrasonic characterization of whole cells and isolated nuclei," Ultrasound Med. Biol. **33**, in press.

Temkin, S. (**1999**). "Radial pulsations of a fluid sphere in a sound wave," J. Fluid Mech. **380**, 1–38.

Waag, R. C. (**1984**). "A review of tissue characterization from ultrasonic scattering," IEEE Trans. Biomed. Eng. **31**(12), 884–893.

Wang, C., Koistinen, P., Yang, G. S., Williams, D. E., Lyman, S. D., Minden, M. D., and McCulloch, E. A. (**1991**). "Mast-cell growth-factor, a ligand for the receptor encoded by c-kit, affects the growth in culture of the blast cells of acute myeloblastic-leukemia," Leukemia **5**(6), 493–499.